

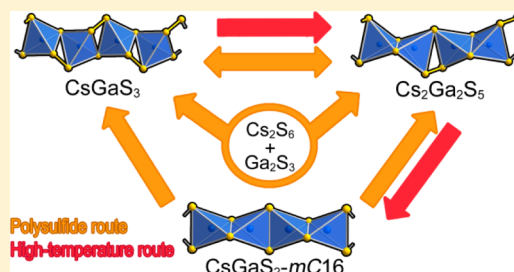
Interconversion of One-Dimensional Thiogallates $\text{Cs}_2[\text{Ga}_2(\text{S}_2)_{2-x}\text{S}_{2+x}]$ ($x = 0, 1, 2$) by Using High-Temperature Decomposition and Polysulfide-Flux Reactions

Daniel Friedrich,¹ Marc Schlosser, and Arno Pfitzner^{*1}

Institut für Anorganische Chemie, Universität Regensburg, Universitätsstraße 31, 93040 Regensburg, Germany

Supporting Information

ABSTRACT: The potential of cesium polysulfide-flux reactions for the synthesis of chalcogenogallates was investigated by using X-ray diffraction and Raman spectroscopy. An investigation of possible factors influencing the product formation revealed that only the polysulfide content x in the Cs_2S_x melts has an influence on the crystalline reaction product. From sulfur-rich melts ($x > 7$), CsGaS_3 is formed, whereas sulfur-poor melts ($x < 7$) lead to the formation of $\text{Cs}_2\text{Ga}_2\text{S}_5$. *In situ* investigations using high-temperature Raman spectroscopy revealed that the crystallization of these solids takes place upon cooling of the melts. Upon heating, CsGaS_3 and $\text{Cs}_2\text{Ga}_2\text{S}_5$ release gaseous sulfur due to the degradation of S_2^{2-} units. This decomposition of CsGaS_3 to $\text{Cs}_2\text{Ga}_2\text{S}_5$ and finally to $\text{CsGaS}_2\text{-}m\text{C16}$ was further studied *in situ* by using high-temperature X-ray powder diffraction. A combination of the polysulfide reaction route and the high-temperature decomposition leads to the possibility of the directed interconversion of these thiogallates. The presence of disulfide units in the anionic substructures of these thiogallates has a significant influence on the electronic band structures and their optical properties. This influence was studied by using UV/vis-diffuse reflectance spectroscopy and DFT simulations, revealing a trend of smaller band gaps with increasing S_2^{2-} content.



adjusting the sulfur content, as shown by Dürichen and Bensch¹⁵ as well as by Palchik et al.¹⁶

In this paper, we report on the facilitated synthesis of the thiogallates $\text{Cs}_2\text{Ga}_2\text{S}_5$ ⁵ and CsGaS_3 ³, as well as the reactivity of thiogallates in molten polysulfide fluxes and at elevated temperatures. In order to elucidate the product formation in the polysulfide melts, the reactions were investigated *in situ* by high-temperature Raman spectroscopy. The high-temperature degradation processes of CsGaS_3 and $\text{Cs}_2\text{Ga}_2\text{S}_5$ were further studied *in situ* by high-temperature X-ray diffraction techniques. Furthermore, the optical properties and the influence of disulfide units on the band gaps of these semiconductors were investigated by UV/vis-diffuse reflectance spectroscopy and DFT calculations.

RESULTS AND DISCUSSION

As the following investigations all involve the three thiogallates CsGaS_3 ³, $\text{Cs}_2\text{Ga}_2\text{S}_5$ ⁵, and $\text{CsGaS}_2\text{-}m\text{C16}$ ¹⁷, the crystal structures of these solids will be briefly discussed beforehand. Crystallographic data of these substances are listed in Table 1. All three compounds feature polymeric anionic chains as displayed in Figure 1. These chains can be converted into each other by substitution of chalcogenide ions by dichalcogenide ions

INTRODUCTION

Group 13 chalcogenometallates containing alkali metal cations $M_xT_yQ_z$ (M = alkali metal, T = triel, Q = chalcogen) are interesting materials due to their semiconducting properties. These materials are used, e.g., in gas sensors or detectors for high-energy radiation.¹ The crystal structures of most compounds in the ternary systems $M\text{-}T\text{-}Q$ consist of oligomeric or polymeric one-, two-, or three-dimensional (1D, 2D, 3D) anions formed by condensed TQ_4 tetrahedra.² Among the large number of chalcogenotriellates, however, only a few compounds featuring polychalcogenide units are known. Incorporation of polychalcogenide units into the anionic structures leads to more exotic structural motives. The crystal structures of mixed-valent chalcogenometallates like CsGaQ_3 ,^{3,4} $\text{Cs}_2\text{Ga}_2\text{Q}_5$,^{5,6} CsAlTe_3 ⁷ and several chalcogenoborates^{8–11} show 1D anionic chains containing Q_2^{2-} or Q_3^{2-} units ($Q = \text{S}, \text{Se}$). The mixed-valent nature of the chalcogen in these compounds should significantly influence the properties of these semiconductors. Therefore, it is necessary to understand the reactive behavior of these compounds and the conditions necessary for their formation in order to design compounds with desired properties. Molten polysulfide fluxes are an established method for the synthesis of substances featuring polysulfide anions.^{12–14} Due to an enhanced diffusion rate at comparably low temperatures in these fluxes, the formation of thermodynamically metastable compounds is favored as compared to high-temperature reactions. Furthermore, the properties of these fluxes (basicity, viscosity, etc.) can be fine-tuned by

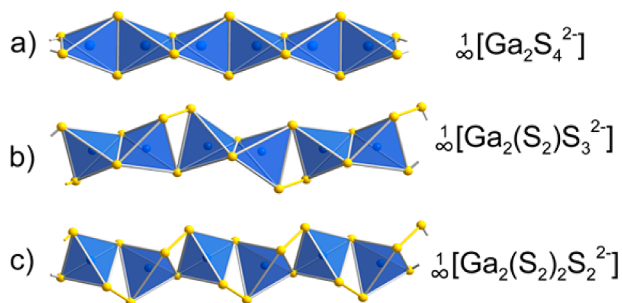
Received: June 16, 2017

Revised: July 19, 2017

Published: July 31, 2017

Table 1. Crystallographic Data for CsGaS₃,³ Cs₂Ga₂S₅,⁵ and CsGaS₂-mC16¹⁷

	CsGaS ₃	Cs ₂ Ga ₂ S ₅	CsGaS ₂ -mC16
crystal system	monoclinic	monoclinic	monoclinic
space group	<i>P</i> 2 ₁ / <i>c</i>	<i>C</i> 2/ <i>c</i>	<i>C</i> 2/ <i>c</i>
<i>a</i> /Å	7.558(3)	12.586(1)	7.388(1)
<i>b</i> /Å	12.502(7)	7.143(1)	12.128(1)
<i>c</i> /Å	6.411(5)	12.344(1)	5.899(1)
<i>β</i> /deg	107.75(4)	108.34(1)	113.21(1)
<i>V</i> /Å ³	576.9(6)	1053.6(1)	458.8(3)
<i>Z</i>	4	4	4
<i>ρ</i> /g·cm ⁻³	3.440	3.564	3.647

**Figure 1.** Polymeric thiogallate chains in (a) CsGaS₂-mC16, (b) Cs₂Ga₂S₅, and (c) CsGaS₃.

according to the formula $\frac{1}{\infty}[\text{Ga}_2(\text{S}_2)_{2-x}\text{S}_{2+x}^{2-}]$ ($x = 0, 1, 2$). The cesium cations in all three compounds form a cubic diamond analogous topology.^{3,5,17}

During our investigations of the formation of Cs₂Ga₂S₅, we noticed that the crystallization of the product seemed to be favored by the *in situ* formation of cesium polysulfides when using the alkali metal azide route.⁵ This polysulfide was identified as Cs₂S₆ by Raman spectroscopy (see the Supporting Information, Figure S1). After removal of the polysulfide with *N,N'*-dimethylformamide (DMF), the powdered samples always contained traces of gallium sulfide as impurities. Furthermore, we never managed to prepare a sample of CsGaS₃ by using the alkali metal azide route^{5,6,17} or an exact reproduction of the polysulfide-flux synthesis described by Suseela Devi et al.³ Usage of the alkali azide route always resulted in the formation of CsGaS₂-mC16. Therefore, we systematically investigated the synthesis of thiogallates using cesium polysulfide melts.

Polysulfide-Flux Reactions. On the basis of the observation that Cs₂S₆ is involved in the formation of Cs₂Ga₂S₅, we decided to investigate mixtures of Cs₂S₆ and different gallium sources (Ga, GaS, Ga₂S₃) with different stoichiometric ratios. These samples were annealed in evacuated quartz glass ampules at 530 °C for 7 days analogous to our synthesis of Cs₂Ga₂S₅.⁵ The excess polysulfide was then removed by using DMF or acetone and water. Other batches of the same reaction mixtures were annealed at different temperatures between 300 and 500 °C in order to investigate the influence of the temperature.

Ex Situ Investigations. After removal of the excess polysulfide, the dried samples were characterized by using powder X-ray diffraction. Interestingly, the crystalline reaction product in all samples was either Cs₂Ga₂S₅ or CsGaS₃. As the same results were obtained regardless of the annealing temperature, the decisive factor for the product formation

had to be the stoichiometric composition of the melt. It should be noted, however, that higher temperatures lead to a faster quantitative conversion of the gallium source. Similar investigations of niobates¹⁵ and germanates¹⁶ revealed that the length of the polysulfide chain *x* in the Cs₂S_{*x*} melt, specifically the ratio Cs₂S/*S*, is important for the product formation. This fact is also true for the synthesis of the thiogallates under discussion; see Table S1 of the Supporting Information.

The ratio Cs₂S_{*x*}/Ga has no influence on the crystalline reaction product, since gallium is consumed as long as it is available. Therefore, any gallium source can be chosen as long as the Cs₂S/*S* ratio of the melt remains correct. To further test this assumption, additional sulfur was added to the “sulfur-poor” mixtures originally leading to Cs₂Ga₂S₅. For the mixtures with a Cs₂S/*S* ratio < 0.143(2), CsGaS₃ was formed instead of Cs₂Ga₂S₅, further confirming the importance of the polysulfide content (more specifically, the basicity and oxidation power) of the melts.

On the basis of this knowledge, the possibility of a direct conversion of CsGaS₂ or Cs₂Ga₂S₅ to CsGaS₃ was tested. For that purpose, new mixtures of Cs₂S₆ and the ternary compounds were prepared (see Table S1). Additional sulfur had to be added in order to bring the ratio Cs₂S/*S* below 0.14. The samples were annealed at 500 °C for 7 days. Once again, the formation of CsGaS₃ was observed in the sulfur-rich melts (Cs₂S/*S* < 0.143), whereas Cs₂Ga₂S₅ was obtained from the sulfur-poor mixtures (Cs₂S/*S* > 0.143). The same observation was made using either polymorph of CsGaS₂ as gallium source for the polysulfide fluxes.

In Situ X-ray Investigations. We employed diffraction techniques in order to investigate the processes in the molten polysulfides, especially the formation of the crystalline products, *in situ*. A study of the reaction using high-temperature X-ray powder diffraction, however, failed due to technical difficulties. These measurements were performed on a STOE Stadi P diffractometer equipped with a capillary furnace, and a capillary in vertical orientation. Upon melting, the samples moved out of the incident X-ray beam and were thus no longer accessible for the *in situ* experiments. We therefore decided to use a different approach after encountering these difficulties.

In Situ Raman Spectroscopy. Raman spectroscopy turned out to be a suitable technique to study the processes in cesium polysulfide melts. The unambiguous assignment of the observed vibrational frequencies was possible since all crystalline compounds (Cs₂S₆, Ga₂S₃, CsGaS₂-mC16, Cs₂Ga₂S₅, and CsGaS₃) could be characterized beforehand (see the Supporting Information, Figures S2–S5). The spectra for Cs₂Ga₂S₅ (Figure S2) and CsGaS₂-mC16 (Figure S3) are identical to our previously reported spectra.^{5,17} No Raman spectrum of CsGaS₃ (Figure S4) has been published prior to this work. The vibration spectra of Cs₂S₆ (Figure S5) are in good agreement with the values reported by Ziemann et al.¹⁸ and the calculations performed by Steudel et al.¹⁹ Furthermore, we were able to overcome the difficulties observed in the X-ray diffraction experiments by constructing a special heatable sample holder. This holder allowed the usage of the same quartz glass ampules, which were used for the *ex situ* investigations (diameter 5 mm). A construction scheme of the sample holder and the spectrometer are shown in the Supporting Information in Figures S6 and S7. Details on the components in the spectrometer are given in the Experimental Section.

The main goal of these *in situ* experiments was to determine the moment the crystalline reaction product is formed (upon heating, during the annealing, upon cooling, etc.). Furthermore, we wanted to study the formation of small building blocks, i.e., GaS_4^{5-} tetrahedra, in the melt prior to crystallization. The investigated samples were binary mixtures of Cs_2S_6 and Ga_2S_3 with a stoichiometric ratio of 2:1 and 5:1. These mixtures reproducibly yielded CsGaS_3 and $\text{Cs}_2\text{Ga}_2\text{S}_5$, respectively. The starting materials were thoroughly ground to ensure optimum intermixture. Furthermore, the experiments were performed in the temperature region from 20 to 400 °C. This procedure should not affect the final product as the *ex situ* experiments showed. During all three stages of the polysulfide reaction (heating, annealing, and cooling), several Raman spectra were measured. No change of the vibrational bands was observed upon heating of the powdered samples below the melting point of Cs_2S_6 . Above the melting point of Cs_2S_6 , only weak bands of vibrations assigned to Ga_2S_3 were detected. The general shape of the spectrum did not change during annealing of the samples at 400 °C. After 24 h, the heater was turned off and spectra were measured in intervals of 1 min (temperature was manually registered). The excessive molten polysulfide started to crystallize, and the corresponding vibrational bands of Cs_2S_6 were observed during this cooling period. The spectra, however, contained additional vibrational bands not originating from either Cs_2S_6 or Ga_2S_3 (Figure 2). A comparison of the Raman spectra of the reaction mixture ($\text{Cs}_2\text{S}_6 + \text{Ga}_2\text{S}_3$) with the spectra of the pure product phases revealed that crystalline CsGaS_3 and $\text{Cs}_2\text{Ga}_2\text{S}_5$ were formed in the respective sample (Figure 2). X-ray diffraction patterns of the samples showed an almost complete conversion of the gallium source, as only weak reflections of residual Ga_2S_3 were observed. This is likely due to the relatively short reaction times during the experiments, as pure samples could be obtained after longer annealing.

The Raman spectroscopic investigations revealed no additional details on the processes taking place in the polysulfide melts. However, we managed to identify one important fact of these polysulfide-flux reactions. The crystalline product $\text{Cs}_2\text{Ga}_2\text{S}_5$ or CsGaS_3 does not form during annealing of the polysulfide melt. The product rather crystallizes upon cooling below the melting point of the flux. Due to the increasing intensities of the product bands in the course of cooling, one can assume that the amount of the product phase increases.

Summary. The directed synthesis of the thiogallates $\text{Cs}_2\text{Ga}_2\text{S}_5$ and CsGaS_3 is possible in cesium polysulfide fluxes. The crucial parameter determining which of these two products is formed is the length of the polysulfide chains x in the Cs_2S_x melts. This is represented by the ratio $\text{Cs}_2\text{S}_x/\text{S}$ (Table S1). The chosen gallium source has no influence on the crystalline reaction product. Therefore, even the conversion of ternary compounds like CsGaS_2 is possible. Furthermore, the yield is only limited by the amount of the gallium source, as long as enough cesium polysulfide is provided.

High-Temperature Degradation. After the successful preparation of pure samples of $\text{Cs}_2\text{Ga}_2\text{S}_5$ and CsGaS_3 , we decided to study the thermal behavior of these compounds. A differential thermal analysis (DTA) was performed in order to determine the melting points of these compounds. However, no thermal effect was observed in the temperature region from 20 to 1000 °C in both cases. However, it is quite unlikely that polymeric thiogallates with disulfide units are stable to such high temperature. Therefore, we investigated the substances using high-temperature X-ray powder diffraction techniques.

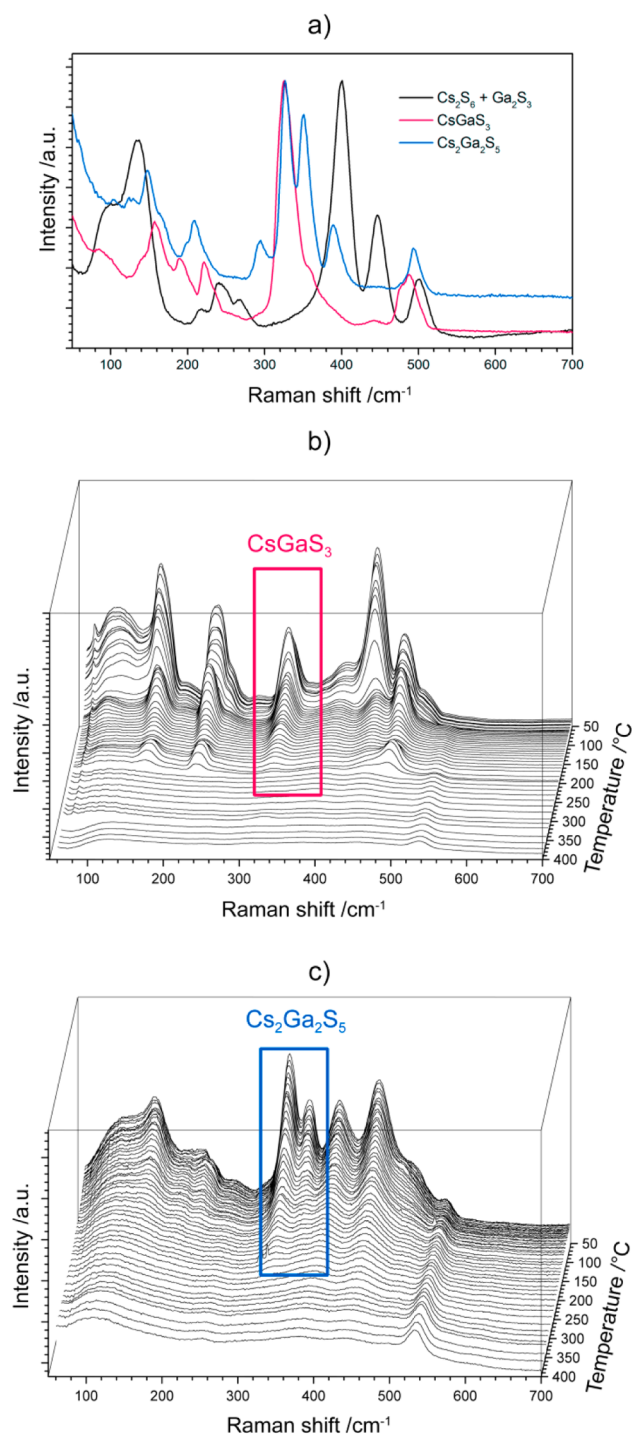


Figure 2. (a) Comparison of the Raman spectra of the reaction mixture ($\text{Cs}_2\text{S}_6 + \text{Ga}_2\text{S}_3$) with the spectra of pure CsGaS_3 and $\text{Cs}_2\text{Ga}_2\text{S}_5$, respectively. (b) Series of measurements during cooling of a mixture of $\text{Cs}_2\text{S}_6:\text{Ga}_2\text{S}_3 = 2:1$. (c) Series of measurements during cooling of a mixture of $\text{Cs}_2\text{S}_6:\text{Ga}_2\text{S}_3 = 5:1$. The weak peak at $\sim 540 \text{ cm}^{-1}$ results from the sample holder or the spectrometer and is present in all spectra.

After the experiments, small amounts of elemental sulfur could be observed in all capillaries. Upon heating, a change in the diffraction pattern of both compounds can be observed. The full decomposition pathway can be observed for the compound CsGaS_3 (Figure 3).

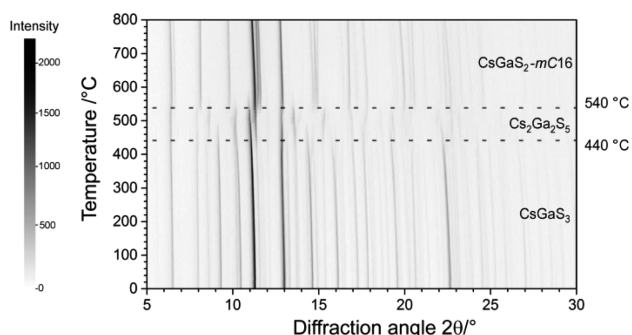


Figure 3. Evolution of the X-ray powder pattern during thermal decomposition of CsGaS_3 in the temperature region from 20 to 800 °C (Mo- $K\alpha_1$ radiation).

The compound starts to decompose to $\text{Cs}_2\text{Ga}_2\text{S}_5$ at temperatures above ca. 400 °C. $\text{Cs}_2\text{Ga}_2\text{S}_5$ is the sole detectable crystalline phase in the temperature region from 440 to 540 °C. If the temperature is raised above 540 °C, the compound decomposes to $\text{CsGaS}_2\text{-mC16}$. This phase is stable up to the melting point of about 1130 °C.¹⁷ One sulfur atom of the disulfide units S_2^{2-} is removed from the anionic chains during each degradation step. Even though the crystal structures of CsGaS_3 , $\text{Cs}_2\text{Ga}_2\text{S}_5$, and $\text{CsGaS}_2\text{-mC16}$ seem to be related (Table 1), it is not possible to transform the atomic sites of the three structures using allowed crystallographic transformations. Furthermore, no intermediate crystalline or amorphous phase was detected.

The high-temperature decomposition of CsGaS_3 was also investigated in the temperature region from 25 to 800 °C by using thermogravimetric analysis (TGA). This analysis also revealed a two-step degradation of the compound (Supporting Information, Figure S8) with weight losses of 4.6% and 7.1% (calculated loss of 1 equiv of $\text{S} = 5.3\%$ based on the mass of CsGaS_3). The temperatures for the thermal degradation of CsGaS_3 determined by different methods slightly differ, which is attributed to different heating rates and experimental environments.

Overview. When the results of the polysulfide-flux syntheses and the high-temperature decomposition are combined, a “cycle” for the interconversion of the compounds $\text{CsGaS}_2\text{-mC16}$, $\text{Cs}_2\text{Ga}_2\text{S}_5$, and CsGaS_3 can be drawn (Figure 4).

Optical Properties. The optical band gaps of the thiogallates CsGaS_3 , $\text{Cs}_2\text{Ga}_2\text{S}_5$, and $\text{CsGaS}_2\text{-mC16}$ were reported as 3.00,³ 3.26,⁵ and 3.27 eV,¹⁷ respectively. During

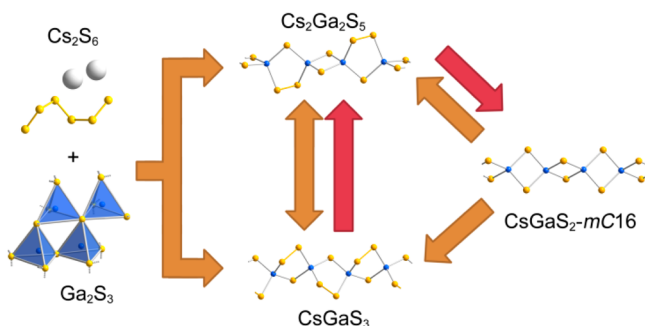


Figure 4. Schematic representation of the different possibilities of interconversion of the thiogallates CsGaS_3 , $\text{Cs}_2\text{Ga}_2\text{S}_5$, and $\text{CsGaS}_2\text{-mC16}$ using the high-temperature decomposition route (red arrows) and the polysulfide route (orange arrows).

our investigations, however, we used our newly attained knowledge on the synthesis of these thiogallates, and we prepared pure samples of these compounds. Optical band gaps were thus redetermined by diffuse reflectance spectroscopy. The absorption data were calculated using a modified Kubelka–Munk function (Figure S9).²⁰ Table 2 lists the band gaps of all three compounds.

Table 2. Experimental Optical Band Gaps of CsGaS_3 , $\text{Cs}_2\text{Ga}_2\text{S}_5$, and $\text{CsGaS}_2\text{-mC16}$.¹⁷ The Calculated Gaps (DFT, GGA) Are Also Listed

compound	experimental value (eV)	calculated value (eV)
CsGaS_3	2.78	2.24
$\text{Cs}_2\text{Ga}_2\text{S}_5$	2.91	2.69
$\text{CsGaS}_2\text{-mC16}$ ¹⁷	3.27	3.34

We previously reported a value of 3.26 eV for the band gap of $\text{Cs}_2\text{Ga}_2\text{S}_5$, which most likely resulted from impurities of $\text{CsGaS}_2\text{-mC16}$. This can be explained with a partial decomposition of the sample upon annealing at 530 °C.⁵ The reported optical band gap of 3.00 eV for CsGaS_3 by Suseela Devi et al. possibly originates from $\alpha\text{-Ga}_2\text{S}_3$ (see Figure S10), which was used as a starting material for the synthesis of CsGaS_3 .³

The electronic structures of these thiogallates were analyzed by relativistic DFT calculations using the generalized gradient approximation (GGA) according to Perdew–Burke–Ernzerhof (PBE).²¹ For the total energy and band structure calculations based on the experimentally determined structures, the full-potential local orbital code FPLO was applied.²² The calculated band gaps are listed in Table 2. The orbital projected density of states (PDOS) for CsGaS_3 , $\text{Cs}_2\text{Ga}_2\text{S}_5$, and $\text{CsGaS}_2\text{-mC16}$ is shown in Figure 5. As the bonding behavior in $\text{Cs}_2\text{Ga}_2\text{S}_5$ and $\text{CsGaS}_2\text{-mC16}$ was already discussed beforehand,^{5,17} only a brief comparison shall be presented.

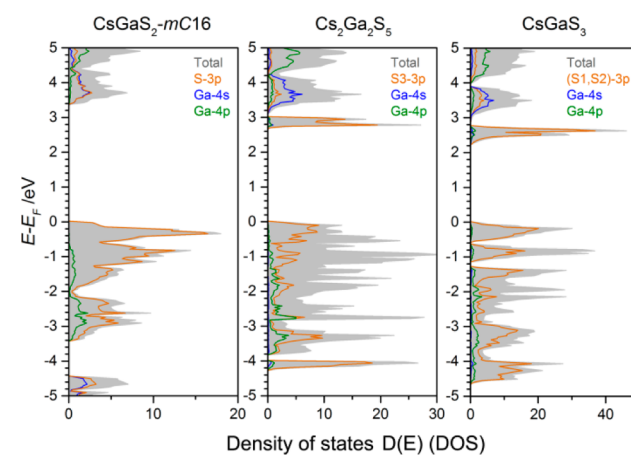


Figure 5. Calculated total (TDOS, gray) and partial density of states (PDOS) for $\text{CsGaS}_2\text{-mC16}$, $\text{Cs}_2\text{Ga}_2\text{S}_5$, and CsGaS_3 .

The bonding character of Cs in these compounds is mainly ionic, which can be concluded from the unoccupied Cs-6s states. Therefore, the alkali metal does not influence the band gap in these structures. Ga–S interactions within the GaS_4 tetrahedra of all three thiogallates cause a splitting into valence and conduction band. The band gaps are mostly determined by the energies of the S-3p states. The influence of the sulfur ions

becomes obvious in those compounds containing S_2^{2-} units like $CsGaS_3$ and $Cs_2Ga_2S_5$. Due to the reduced charge of sulfur in these disulfide ions, the Ga–S interactions are weaker as compared to $CsGaS_2-mC16$. Therefore, longer distances $d(\text{Ga–S})$ between Ga^{3+} and the disulfide sulfur atoms are observed in these compounds.^{3,5,17} These weaker interactions cause a shrinking of the band gap as soon as S_2^{2-} units are present in the polymeric anionic chain. An increasing amount of the disulfide anions, however, only slightly further lowers the band gap. This observation suggests tailoring the band gap of these compounds by preparing the solid solutions series $Cs_xGa_2S_{4+x}$ ($x = 0–2$). Investigations of this solid solution series, however, always resulted in a phase separation into the boundary phases $CsGaS_3$, $Cs_2Ga_2S_5$, and $CsGaS_2$, respectively.

CONCLUSION

In this work, we explored the application of cesium polysulfide fluxes for the synthesis of cesium thiogallates. During the explorative syntheses, we discovered that the formation of $CsGaS_3$ and $Cs_2Ga_2S_5$ is solely dependent on the polysulfide content (more specifically, the basicity and oxidation power) in these melts. The chosen gallium source does not play any role, as elemental gallium, and appropriate binary or ternary compounds all lead to the same result. Using high-temperature Raman spectroscopy, we determined that the reaction product in these melts crystallizes during cooling of the reaction mixtures. The formation of gaseous sulfur can be observed upon heating of $CsGaS_3$ and $Cs_2Ga_2S_5$. An analysis of this degradation process using high-temperature X-ray powder diffraction revealed a two-step transformation from $CsGaS_3$ to $Cs_2Ga_2S_5$ and finally to $CsGaS_2-mC16$. One disulfide unit of the anionic thiogallate chains is degraded in the course of each decomposition step. On the basis of this knowledge, it is now possible to interconvert $CsGaS_2-mC16$, $Cs_2Ga_2S_5$, and $CsGaS_3$ using the polysulfide-flux or high-temperature decomposition route. The influence of the disulfide ions on the band gaps of these compounds was further studied by UV/vis spectroscopy and DFT calculations, revealing a trend of smaller band gaps with increasing S_2^{2-} content in the anionic chains.

EXPERIMENTAL SECTION

Synthesis of the Starting Materials. Gallium sulfide Ga_2S_3 was synthesized by annealing of gallium (Chempur 99.99%) and sulfur (Chempur 99.999%) at 1000 °C for several days. Powdered samples of Cs_2S_6 were prepared by reaction of stoichiometric amounts of sulfur with an ethanolic solution of Cs_2S , which was obtained by passing H_2S into an ethanolic solution of $CsOH \cdot H_2O$ (Alfa Aesar 99.9%).

X-ray Powder Diffraction. The X-ray powder diffraction experiments were performed on a STOE STADI P diffractometer equipped with a Dectris Mythen 1K detector and a high-temperature capillary furnace. Monochromatized $Mo-K\alpha_1$ radiation ($\lambda = 0.70930$ Å) was used in all experiments. The WinX^{POW} software package from STOE & Cie²³ was used for data collection and processing. For the high-temperature measurements, powdered samples were loaded in quartz capillaries (diameter 0.3 mm) and investigated in the temperature region from 20 to 800 °C in steps of 10 °C ($5.00^\circ < 2\theta < 30.00^\circ$; irradiation time: 10 min per diffraction pattern). The capillaries were held at the respective temperature for 3 min prior to each measurement. The furnace temperature was controlled by a Eurotherm 24.16 controller ($\Delta T = \pm 1$ °C).

Raman spectroscopy. The high quality Raman spectra shown in the Supporting Information were recorded on a DXR SmartRaman Spectrometer from Thermoscientific (excitation wavelength $\lambda = 532$ nm) in the range of 50–1000 cm^{-1} with a resolution of 0.5 cm^{-1} (irradiation time: 1 s, 10 repetitions per spectrum). The high-

temperature *in situ* Raman experiments were performed on a self-assembled spectrometer by Prof. Alkwin Slenczka. The spectrometer is equipped with an Oriel MS 260i spectrograph and an Andor DB401-UV CCD camera. The spectra were measured in backscattering geometry. The laser light (He-Ne laser, $\lambda = 632$ nm) was focused on the sample by a microscope objective (Olympus LMPLFL 50x/0.5). Rayleigh scattering or laser reflections were filtered out by a notch filter. The self-constructed sample holder is composed of an infrared radiant heater (RS components GmbH, 500 W, max. 750 °C) inside a steel chamber (see Figure S6). The sample temperature was measured with a Eurotherm 21.16 controller ($\Delta T = \pm 1$ °C).

Thermogravimetric Analysis. The thermogravimetric analysis was performed with a SETARAM TG-DTA 92.16.18. A small amount of the powdered sample was heated in a corundum crucible (heating rate: 10 °C/min) in an argon stream.

UV/vis Spectroscopy. Diffuse reflectance measurements were performed with a Bruins Omega 20 UV/vis spectrometer using $BaSO_4$ as a reference (100% reflectance). The absorption data were calculated using a modified Kubelka–Munk function.²⁰

DFT Calculations. The first-principles calculations were carried out within the framework of density functional theory (DFT) with exchange-correlation functionals in the generalized gradient approximation (GGA) according to Perdew–Burke–Ernzerhof (PBE).²¹ The full potential local orbital code FPLO14²² was applied for total energy and band structure calculations based on the experimentally obtained structures. A k -grid mesh of $12 \times 12 \times 12$ was used. The calculations converged with a maximum divergence of $< 10^{-7}$ Hartree.

ASSOCIATED CONTENT

Supporting Information

The Supporting Information is available free of charge on the ACS Publications website at DOI: 10.1021/acs.cgd.7b00840.

Overview of selected polysulfide reaction mixtures, Raman spectra of pure $CsGaS_3$, $Cs_2Ga_2S_5$, and $CsGaS_2-mC16$, infrared and Raman spectra of Cs_2S_6 , schematic illustration of the *in situ* Raman sample holder, thermogravimetric analysis of $CsGaS_3$, optical band gaps of $CsGaS_2-mC16$, $Cs_2Ga_2S_5$, $CsGaS_3$, and $\alpha-Ga_2S_3$ (PDF)

AUTHOR INFORMATION

Corresponding Author

*E-mail: arno.pfitzner@chemie.uni-regensburg.de.

ORCID

Daniel Friedrich: 0000-0001-6953-8114

Arno Pfitzner: 0000-0001-8653-7439

Notes

The authors declare no competing financial interest.

ACKNOWLEDGMENTS

The authors would like to thank Prof. Dr. Alkwin Slenczka (University of Regensburg) for his great help regarding the *in situ* Raman measurements, as well as his willingness to modify the spectrometer. We would further like to thank Prof. Dr. Manfred Scheer (University of Regensburg) for the high quality Raman measurements at ambient conditions.

REFERENCES

- (1) Androulakis, J.; Peter, S. C.; Malliakas, C. D.; Peters, J. A.; Liu, Z.; Wessels, B. W.; Song, J.-H.; Jin, H.; Freeman, A. J.; Kanatzidis, M. G.; Li, H. *Adv. Mater.* **2011**, *23*, 4163–4167.
- (2) Krebs, B. *Angew. Chem.* **1983**, *95*, 113–134.
- (3) Suseela Devi, M.; Vidyasagar, K. *J. Chem. Soc., Dalton Trans.* **2002**, 4751–4754.

- (4) Do, J.; Kanatzidis, M. G. *Z. Anorg. Allg. Chem.* **2003**, *629*, 621–624.
- (5) Friedrich, D.; Pielhofer, F.; Schlosser, M.; Weihrich, R.; Pfitzner, A. *Chem. - Eur. J.* **2015**, *21*, 1811–1817.
- (6) Friedrich, D.; Schlosser, M.; Pfitzner, A. *Z. Anorg. Allg. Chem.* **2014**, *640*, 826–829.
- (7) Eisenmann, B.; Jäger, J. *Z. Kristallogr.* **1991**, *197*, 251–252.
- (8) Püttmann, C.; Hiltmann, F.; Hamann, W.; Brendel, C.; Krebs, B. *Z. Anorg. Allg. Chem.* **1993**, *619*, 109–116.
- (9) Hammerschmidt, A.; Küper, J.; Stork, L.; Krebs, B. *Z. Anorg. Allg. Chem.* **1994**, *620*, 1898–1904.
- (10) Lindemann, A.; Küper, J.; Jansen, C.; Kuchinke, J.; Köster, C.; Hammerschmidt, A.; Dösch, M.; Pruß, T.; Krebs, B. *Z. Anorg. Allg. Chem.* **2001**, *627*, 419–425.
- (11) Lindemann, A.; Küper, J.; Hamann, W.; Kuchinke, J.; Köster, C.; Krebs, B. *J. Solid State Chem.* **2001**, *157*, 206–212.
- (12) Scheel, H. J. *J. Cryst. Growth* **1974**, *24–25*, 669–673.
- (13) Kanatzidis, M. G. *Chem. Mater.* **1990**, *2*, 353–363.
- (14) Sunshine, S. A.; Kang, D.; Ibers, J. A. *J. Am. Chem. Soc.* **1987**, *109*, 6202–6204.
- (15) Dürichen, P.; Bensch, W. *Z. Naturforsch.* **2002**, *57b*, 1382–1386.
- (16) Palchik, O.; Marking, G. M.; Kanatzidis, M. G. *Inorg. Chem.* **2005**, *44*, 4151–4153.
- (17) Friedrich, D.; Schlosser, M.; Weihrich, R.; Pfitzner, A. *Inorg. Chem. Front.* **2017**, *4*, 393–400.
- (18) Ziemann, H.; Buss, W. *Z. Anorg. Allg. Chem.* **1979**, *455*, 69–87.
- (19) Steudel, R.; Schuster, F. *Z. Naturforsch.* **1977**, *32a*, 1313–1319.
- (20) Kisch, H. *Angew. Chem., Int. Ed.* **2013**, *52*, 812–847.
- (21) Perdew, J. P.; Burke, K.; Ernzerhof, M. *Phys. Rev. Lett.* **1996**, *77*, 3865–3868.
- (22) Koepernik, K.; Eschrig, H. *Phys. Rev. B: Condens. Matter Mater. Phys.* **1999**, *59*, 1743–1757.
- (23) WinX^{POW}, Version 3; STOE & Cie GmbH: Darmstadt, Germany, 2014.